Tidal Deformability from GW170817 as a Direct Probe of the Neutron Star Radius

Item Type	Article
Authors	Raithel, Carolyn A.; Özel, Feryal; Psaltis, Dimitrios
Citation	Carolyn A. Raithel et al 2018 ApJL 857 L23
DOI	10.3847/2041-8213/aabcbf
Publisher	IOP PUBLISHING LTD
Journal	ASTROPHYSICAL JOURNAL LETTERS
Rights	© 2018. The American Astronomical Society. All rights reserved.
Download date	27/08/2022 11:04:40
Item License	http://rightsstatements.org/vocab/InC/1.0/
Version	Final published version
Link to Item	http://hdl.handle.net/10150/627756

CrossMark

Tidal Deformability from GW170817 as a Direct Probe of the Neutron Star Radius

Carolyn A. Raithel , Feryal Özel, and Dimitrios Psaltis
Department of Astronomy and Steward Observatory, University of Arizona, 933 N. Cherry Avenue, Tucson, AZ 85721, USA
Received 2018 March 19; revised 2018 April 6; accepted 2018 April 8; published 2018 April 24

Abstract

Gravitational waves from the coalescence of two neutron stars were recently detected for the first time by the LIGO–Virgo Collaboration, in event GW170817. This detection placed an upper limit on the effective tidal deformability of the two neutron stars and tightly constrained the chirp mass of the system. We report here on a new simplification that arises in the effective tidal deformability of the binary, when the chirp mass is specified. We find that, in this case, the effective tidal deformability of the binary is surprisingly independent of the component masses of the individual neutron stars, and instead depends primarily on the ratio of the chirp mass to the neutron star radius. Thus, a measurement of the effective tidal deformability can be used to directly measure the neutron star radius. We find that the upper limit on the effective tidal deformability from GW170817 implies that the radius cannot be larger than ~13 km, at the 90% level, independent of the assumed masses for the component stars. The result can be applied generally, to probe the stellar radii in any neutron star–neutron star merger with a measured chirp mass. The approximate mass independence disappears for neutron star–black hole mergers. Finally, we discuss a Bayesian inference of the equation of state that uses the measured chirp mass and tidal deformability from GW170817 combined with nuclear and astrophysical priors and discuss possible statistical biases in this inference.

Key words: equation of state – gravitational waves – stars: neutron

1. Introduction

The first detection of gravitational waves from a neutron star–neutron star merger (GW170817; Abbott et al. 2017a) marks the start of a new era in the study of neutron stars, their associated transient events, and the dense-matter equation of state (EOS). The electromagnetic counterpart that accompanied the event (Abbott et al. 2017b) has confirmed neutron star mergers as the sources of at least some short-duration gamma-ray bursts, as has long been theorized (Eichler et al. 1989; Narayan et al. 1992; Berger 2014), as well as the source of kilonovae, predicted to be powered by the radioactive decay of merger ejecta (Li & Paczyński 1998; Metzger et al. 2010). Information about the component neutron stars and their underlying EOS is encoded in the waveform itself, which was observed by the two LIGO and one Virgo detectors for ~3000 orbital cycles prior to the merger (Abbott et al. 2017a).

Several studies have already placed constraints on fundamental neutron star properties using these observations. For example, Margalit & Metzger (2017) used the combined gravitational-wave and electromagnetic signals to set an upper limit on the maximum neutron star mass, which is a sensitive constraint on the EOS at high densities (Özel & Psaltis 2009). In another work, Rezzolla et al. (2017) inferred the maximum neutron star mass from the event without relying on models of the electromagnetic signal, instead using only the quasi-universal relations that describe neutron stars and simple models of kilonovae.

The observed gravitational waveform can also be used to place direct constraints on the neutron star EOS. In one of the first quantitative studies exploring EOS effects on the waveform from the coalescence of two neutron stars, Read et al. (2009b) showed that a realistic waveform would deviate significantly from a point-particle waveform and that this could be observed with Advanced LIGO. The degree of the deviation depends on the underlying EOS and, as a result, could be used

to differentiate between EOS that differ in radius by only ~1 km (Read et al. 2009b, 2013; Lackey & Wade 2015).

The magnitude of the deviation is strongest at later times in the inspiral and during the merger, i.e., in the phases where numerical relativity would be necessary to model the waveforms. Nevertheless, Flanagan & Hinderer (2008) found that the early phase of the inspiral depends cleanly on a single EOS-dependent parameter: the tidal Love number, λ. The tidal Love number measures the ratio of the star's tidally induced quadrupolar deformation, $Q^{(\mathrm{tid})}$, to the tidal potential caused by a binary companion, $\varepsilon^{(\mathrm{tid})}$, i.e.,

$$\lambda \equiv -\frac{Q^{(\mathrm{tid})}}{\varepsilon^{(\mathrm{tid})}} \tag{1}$$

or, in dimensionless form,

$$\Lambda \equiv \frac{\lambda}{M^5} \equiv \frac{2}{3} k_2^{(\mathrm{tid})} \left(\frac{Rc^2}{GM}\right)^5, \tag{2}$$

where R is the radius of the neutron star and M is its mass. Following the convention of Flanagan & Hinderer (2008), we call $k_2^{(\mathrm{tid})}$ the tidal apsidal constant. The tidal apsidal constant depends both on the equation of state and the compactness (GM/Rc^2) of the particular star. For realistic, hadronic equations of state, $k_2^{(\mathrm{tid})}$ has been constrained to lie in the range ~0.05–0.15 (Hinderer 2008; Hinderer et al. 2010; Postnikov et al. 2010).

The individual Love numbers for the two stars, Λ_1 and Λ_2, cannot be disentangled in the observed gravitational waveform. Instead, what is measured is an effective tidal deformability of the binary, $\widetilde{\Lambda}$, which is a mass-weighted average of Λ_1 and Λ_2 that we describe in detail in Section 2. The expectation is thus that $\widetilde{\Lambda}$ would measure a mass-weighted compactness for the two neutron stars. Similarly, the two component masses are not measured directly, rather the chirp mass is.

We report here on a new simplification that arises in the effective tidal deformability of the binary when the chirp mass is measured accurately. We find that $\widetilde{\Lambda}$ depends primarily on the ratio of the chirp mass to the neutron star radius. Thus, we find that $\widetilde{\Lambda}$ can be used as a direct probe of the neutron star radius, rather than of the compactness as is typically assumed.

In Section 2, we describe the measured properties of GW170817. We show in Section 3 that the effective tidal deformability is approximately independent of the component masses, when the chirp mass is specified. In Section 4, we use the Newtonian limit to show analytically that the mass independence arises from an inherent symmetry in the expression for the effective tidal deformability. Finally, in Section 5, we perform an example Bayesian inference of the neutron star EOS from the measured tidal deformability and chirp mass and a limited number of prior physical constraints and discuss important statistical biases that can occur in such inference schemes.

2. Properties of GW170817

The properties of GW170817 were inferred by matching the observed waveform with a frequency-domain post-Newtonian waveform model (Sathyaprakash & Dhurandhar 1991), with modifications to account for tidal interactions (Vines et al. 2011), point-mass spin–spin interactions (Mikóczi et al. 2005; Arun et al. 2011; Bohé et al. 2015; Mishra et al. 2016), and effects due to spin–orbit coupling (Bohé et al. 2013). The LIGO analysis using these models is summarized in Abbott et al. (2017a) and references therein.

One of the most tightly constrained properties that was inferred is the chirp mass, defined as

$$\mathcal{M}_c = \frac{(m_1 m_2)^{3/5}}{(m_1 + m_2)^{1/5}} = m_1 \frac{q^{3/5}}{(1+q)^{1/5}}, \tag{3}$$

where m_1 and m_2 are the masses of the primary and the secondary neutron stars, respectively, and we have introduced the mass ratio, $q \equiv m_2/m_1$. The chirp mass was constrained to $\mathcal{M}_c = 1.188^{+0.004}_{-0.002}\,M_\odot$ at the 90% confidence level, independent of the particular waveform model or priors chosen (Abbott et al. 2017a).

By assuming low-spin priors, as is consistent with the binary neutron star systems that have been observed in our Galaxy, the component masses were inferred from the chirp mass to lie within the ranges $m_1 \in (1.36, 1.60)\,M_\odot$ and $m_2 \in (1.17, 1.36)\,M_\odot$, with a mass ratio of $q \in (0.7, 1.0)$, all at the 90% confidence level (Abbott et al. 2017a). These masses are consistent with the range of masses observed in other neutron star systems (see Özel & Freire 2016 for a recent review of neutron star mass measurements).

GW170817 also provided constraints on the effective tidal deformability of the system, defined as

$$\widetilde{\Lambda} \equiv \frac{16}{13} \frac{(m_1 + 12m_2)m_1^4 \Lambda_1 + (m_2 + 12m_1)m_2^4 \Lambda_2}{(m_1 + m_2)^5} \tag{4}$$

(Flanagan & Hinderer 2008; Favata 2014). In Equation (2), we saw that the dimensionless tidal Love number depends only on the stellar compactness and the tidal apsidal constant, which in turn depends on the equation of state and compactness. Combining these expressions, we can explicitly write the
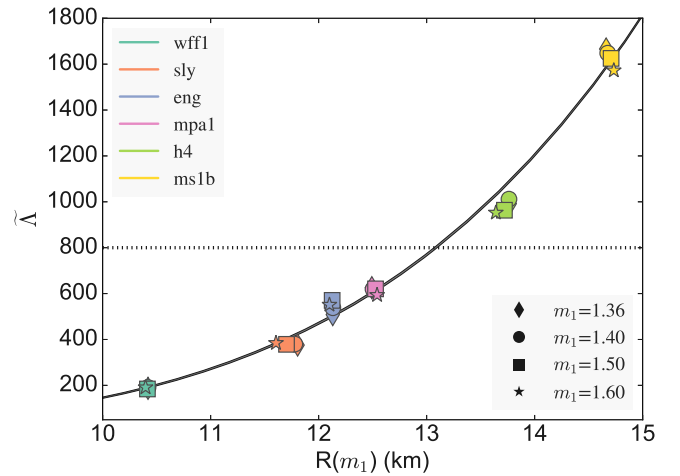
Figure 1. Effective tidal deformability of the binary system as a function of the radius of the primary neutron star. The tidal deformability is calculated for various primary masses (corresponding to the different symbols) using several proposed equations of state (corresponding to the different colors). The mass of the secondary neutron star is found assuming the chirp mass, $\mathcal{M}_c = 1.188\,M_\odot$, from GW170817. The observed 90% confidence upper limit on $\widetilde{\Lambda} \leqslant 800$ is shown as the dotted line. The narrow band (which is indistinguishable from a single curve) shows the range for $q = 0.7$–1.0 from Equation (9). We find that $\widetilde{\Lambda}$ is relatively insensitive to m_1 but scales strongly with radius, and that the upper limit for GW170817 implies $R \lesssim 13$ km.

dependence of the effective tidal deformability on neutron star properties as $\widetilde{\Lambda} = \widetilde{\Lambda}(m_1, m_2, R_1, R_2, \text{EOS})$.

Abbott et al. (2017a) constrain the effective tidal deformability for GW170817 to be $\widetilde{\Lambda} \leqslant 800$ at the 90% confidence level, which disfavors EOS that predict the largest radii stars. In the following analysis, we will show that this measurement can also be used to directly constrain the radii of the individual neutron stars, independently of the component masses.
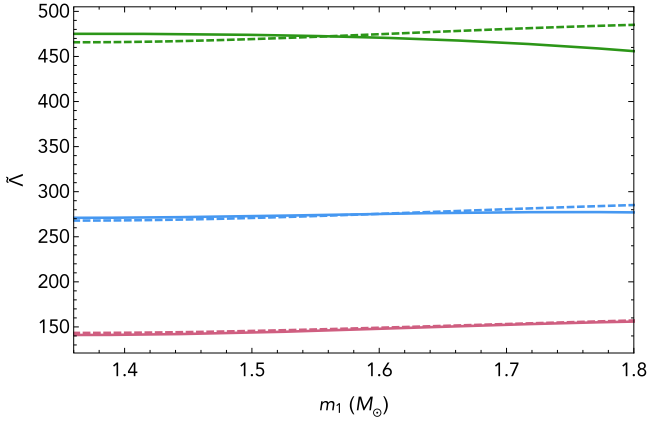
3. Effective Tidal Deformability for GW170817

We start with a simple illustration of our key result. Figure 1 shows the effective tidal deformabilities as a function of the stellar radii for a number of realistic EOS. For each EOS, we calculated these tidal deformabilities for various values of m_1 that lie within the mass range inferred for GW170817 (shown with different symbols). The corresponding values for m_2 are calculated assuming a fixed chirp mass, $\mathcal{M}_c = 1.188\,M_\odot$. The results shown are very similar, whether we use the radius of the primary or the secondary star.

We find that $\widetilde{\Lambda}$ is almost entirely insensitive to the mass of the component stars for the relevant mass range and depends instead primarily on the radius of the star. In particular, $\widetilde{\Lambda}$ changes by nearly an order of magnitude between $R = 10$ km and $R = 15$ km, but, for a given radius, changes negligibly for masses spanning the full range of $m_1 = 1.36$–$1.6\,M_\odot$.

An upper limit of $\widetilde{\Lambda} \lesssim 800$ immediately excludes radii above $\sim$13 km at the 90% confidence level, without requiring detailed knowledge of m_1. As shown in Figure 1, this rules out the EOS that predict the largest radii, such as the hyperonic EOS H4 (Lackey et al. 2006) and the field theoretic nucleonic EOS with a low symmetry energy of 25 MeV, MS1b (Müller & Serot 1996).

The trend found in Figure 1 is for a sample of six EOS. However, this result is more general, as we will now show. It

Figure 2. Effective tidal deformability of the binary system as a function of the primary mass, m_1, when the chirp mass is held fixed at $\mathcal{M}_c = 1.188\,M_\odot$. We calculate $\widetilde{\Lambda}$ for three fixed radii, $R = 10$, 11, and 12 km, shown in purple, blue, and green, respectively. The solid lines show the tidal deformability calculated using the empirically fit universal relation between the tidal deformability of each neutron star and its compactness from Yagi & Yunes (2017), while the dashed lines show the quasi-Newtonian approximation for Λ_i from Equation (7). The quasi-Newtonian approximation is a good approximation to the fully relativistic result.

has been reported previously that the individual tidal deformabilities of neutron stars obey a universal relationship with stellar compactness (Yagi & Yunes 2013). In particular, Yagi & Yunes (2017) found that the relationship can be written as

$$C = a_0 + a_1 \ln\Lambda + a_2 (\ln\Lambda)^2, \qquad (5)$$

where $C \equiv GM/Rc^2$ is the compactness and the coefficients were fit to be $a_0 = 0.360$, $a_1 = -0.0355$, and $a_2 = 0.000705$. The relation holds to within 6.5% for a wide variety of neutron star EOS (Yagi & Yunes 2017).

To see if the trend we have found between $\widetilde{\Lambda}$ and R holds generically for a wide range of EOS, we use the universal relation of Equation (5) to calculate the individual tidal deformabilities, Λ_1 and Λ_2. We then calculate the effective tidal deformability for the binary system, shown as the solid lines in Figure 2 for three different radii. We find that when we use this universal relation to represent a much larger sample of EOS, the trend holds. The effective tidal deformability of the binary depends extremely weakly on the component masses but strongly on the radii of the stars.

The weak dependence of $\widetilde{\Lambda}$ on the component masses is surprising and has not been explored before (see, however, Wade et al. 2014 for an earlier discussion on how $\widetilde{\Lambda}$ can be cast into a radius-like parameter. See also a discussion of the EOS dependence of $\widetilde{\Lambda}$ for a fixed $\mathcal{M}_c$ in Figure 8 of Kawaguchi et al. 2018). This weak dependence on component masses renders $\widetilde{\Lambda}$ a direct probe of the neutron star radius, rather than of the compactness as is typically assumed. We turn now to an analytic explanation of the origin of this result.

4. Effective Tidal Deformability in the Newtonian Limit

In order to see why the dependence on mass in Equation (4) for $\widetilde{\Lambda}$ is so weak, we turn to the Newtonian limit. Yagi & Yunes (2013) showed that the Newtonian expression for the tidal Love number of a star governed by a polytropic EOS with index $n = 1$ (which is appropriate for the majority of realistic

EOS) is simply

$$\Lambda_N = \frac{15 - \pi^2}{3\pi^2} \left(\frac{Rc^2}{Gm} \right)^5. \qquad (6)$$

The full relativistic expression for the tidal deformability of a star is given by Damour & Nagar (2009) for a given compactness and a parameter y, which is the logarithmic derivative of a metric function, H, at the stellar surface. The full expression is far more complicated than what we have introduced so far, but we find that a relatively simple metric correction to Λ_N qualitatively reproduces the universal results computed for more realistic EOS. We call this correction the "quasi-Newtonian" expression and define it as

$$\Lambda_{qN} = \frac{15 - \pi^2}{3\pi^2} \left(\frac{Rc^2}{Gm} \sqrt{1 - \frac{2Gm}{Rc^2}} \right)^5. \qquad (7)$$

This corresponds to Equation (96) of Damour & Nagar (2009) with $\beta \approx 1$. We find that this choice of β produces better agreement with realistic EOS than the exact $n = 1$ polytrope value of $\beta = 3$.

We can combine this with Equation (4) to write the quasi-Newtonian effective tidal deformability as

$$\widetilde{\Lambda}_{qN} = \frac{16}{13} \frac{15 - \pi^2}{3\pi^2} \left(\frac{Rc^2}{Gm_1} \right)^5$$
$$\times \frac{(1 + 12q)\left(1 - \frac{2Gm_1}{Rc^2}\right)^{5/2} + (1 + 12/q)\left(1 - \frac{2Gqm_1}{Rc^2}\right)^{5/2}}{(1+q)^5}, \qquad (8)$$

where we have assumed that the radii for the two neutron stars are the same, as is approximately true for $n = 1$ polytropic EOS. Finally, we can eliminate m_1 in favor of $\mathcal{M}_c$ and q using Equation (3), yielding an expression for $\widetilde{\Lambda}_{qN}$ in terms of only q, $\mathcal{M}_c$, and R.

This quasi-Newtonian form of $\widetilde{\Lambda}_{qN}$ is much simpler to work with, but is it a good enough approximation? We show $\widetilde{\Lambda}$ and $\widetilde{\Lambda}_{qN}$ as functions of m_1 in Figure 2 as the solid and dashed lines, respectively, for fixed radii of $R = 10$, 11, and 12 km and fixed $\mathcal{M}_c = 1.188\,M_\odot$. We find that the quasi-Newtonian approximation provides a reasonable approximation of the full expression for $\widetilde{\Lambda}$, calculated using the quasi-universal relations. We can, therefore, use $\widetilde{\Lambda}_{qN}$ to understand its dependence on the masses.

Expressing $\widetilde{\Lambda}_{qN}$ as a series expansion around $q = 1$, we find

$$\widetilde{\Lambda}_{qN} = \widetilde{\Lambda}_0 (1 + \delta_0 (1 - q)^2) + \mathcal{O}((1-q)^3), \qquad (9)$$

where

$$\widetilde{\Lambda}_0 = \frac{15 - \pi^2}{3\pi^2} \xi^{-5} (1 - 2\xi)^{5/2}, \qquad (10)$$

$$\delta_0 = \frac{3}{104} (1 - 2\xi)^{-2} (-10 + 94\xi - 83\xi^2), \qquad (11)$$

and we have introduced

$$\xi = \frac{2^{1/5} G\mathcal{M}_c}{Rc^2} \qquad (12)$$

as an "effective compactness."

Radius	$\widetilde{\Lambda}_0$	Expansion
$R = 10$ km	143.4	$1 + 0.041\left(\frac{1-q}{1-0.7}\right)^2 + \mathcal{O}\left(\frac{1-q}{1-0.7}\right)^3$
$R = 11$ km	268.0	$1 + 0.029\left(\frac{1-q}{1-0.7}\right)^2 + \mathcal{O}\left(\frac{1-q}{1-0.7}\right)^3$
$R = 12$ km	465.8	$1 + 0.020\left(\frac{1-q}{1-0.7}\right)^2 + \mathcal{O}\left(\frac{1-q}{1-0.7}\right)^3$
$R = 13$ km	764.6	$1 + 0.014\left(\frac{1-q}{1-0.7}\right)^2 + \mathcal{O}\left(\frac{1-q}{1-0.7}\right)^3$

We note that expanding near $q = 1$ is not a restrictive choice. The known population of neutron stars is observed to have a relatively small range of masses and the observed mass distribution of double neutron stars is even narrower, suggesting that most astrophysical merger scenarios will have q near unity (see Özel & Freire 2016).

From Equations (9)–(12), we see that the effective tidal deformability of the binary, $\widetilde{\Lambda}$, scales approximately as R^5 for a given $\mathcal{M}_c$. When the mass ratio is close to unity, the individual masses add only a small correction. For the measured chirp mass of GW170817, we calculate the expansion coefficients for a few radii in Table 1. We note that the mass dependence only enters at order $(1 - q)^2$. Furthermore, the weak dependence on mass becomes even weaker as the radius increases. Even for $R = 10$ km, the mass-dependent term adds at most a $\sim$4% correction to $\widetilde{\Lambda}_{qN}$ for the mass ratio range inferred for GW170817.

We show this quasi-Newtonian expansion for a range of q values, $q \in (0.7, 1.0)$, as the narrow gray band in Figure 1 and find that it does recreate the trend observed in that sample of EOS.

4.1. Black Hole–Neutron Star Mergers

Black hole–neutron star mergers are another source of gravitational waves that may contain information about the neutron star EOS. The tidal Love number of a non-rotating black hole is zero (Binnington & Poisson 2009; Damour & Nagar 2009), which greatly simplifies the effective tidal deformability of Equation (4). However, this simplification also destroys the inherent symmetry in Equation (4), which is the source of the mass independence in the neutron star–neutron star merger scenario. Without this symmetry, a series expansion of $\widetilde{\Lambda}$, as in Equation (9), includes a correction term of order $(1 - q)$.

Due to the lower-order terms of $\mathcal{O}(1 - q)$, there persists a stronger dependence on the mass of the components. Thus, the effective tidal deformability measured from a neutron star–black hole merger does not directly probe the radius, as in the case of a neutron star–neutron star merger. Instead, a measurement of $\widetilde{\Lambda}$ will primarily probe the neutron star compactness.

5. Bayesian Inference of the Radius

In Figure 1, we showed that $\widetilde{\Lambda}$ can be used to directly probe the neutron star radius. The measurement from GW170817 of $\widetilde{\Lambda} \leqslant 800$, at the 90% confidence level, already implies that the radii of the neutron stars should be $\lesssim$13 km. However, in order to place more robust constraints on the neutron star radius or to

place comprehensive constraints on the underlying EOS, we need to incorporate prior physical constraints and other observations within a full Bayesian framework.

Read et al. (2009a) and Özel & Psaltis (2009) introduced the use of piecewise polytropic EOS to convert the observations of neutron stars into constraints on the EOS in a statistically robust way. In Raithel et al. (2016), we showed that an optimal parameterization of the neutron star EOS, given the expected accuracy of measurements in the near future, requires five piecewise polytropes. In Raithel et al. (2017), we further developed the statistical framework with which to perform a Bayesian inference of the pressures of our parametric EOS. In our inference here, we incorporate a variety of astrophysical and nuclear physics priors, including that the EOS is microscopically stable and causal at all pressures, that the lowest two pressures exceed the limit placed by two-nucleon interaction, and that all EOS must produce a neutron star of at least 1.97 $M_\odot$, in order to be within 1σ of the measurements of the most massive neutron stars (Antoniadis et al. 2013; Fonseca et al. 2016). We assume a uniform prior on the pressures. In order not to overparameterize the EOS, while still allowing the possibility of complex behavior to be inferred, we also include a Gaussian regularizer over the second derivative of the pressure ($\lambda = 2$), which penalizes sharp phase transitions. For further details on the setup of our Bayesian inference, see Raithel et al. (2017).

In addition to the above priors, which were extensively studied in Raithel et al. (2017), we also place an *upper* limit on the maximum mass, $M_{\max} < 2.33\ M_\odot$, which is the upper limit of the 90% credibility level found in Rezzolla et al. (2017). This maximum mass was inferred from GW170817 assuming only the quasi-universal neutron star relations and simple models of kilonovae and is thus fairly model independent.

Our goal is to perform a sample Bayesian inference, using the type of data that came from GW170817. Unfortunately, because only an upper limit on $\widetilde{\Lambda}$ was provided by the LIGO–Virgo Collaboration, rather than the full posterior information, we can only perform example inferences at this point.

For the sample inference here, we take the constraint on $\widetilde{\Lambda} \leqslant 800$ to correspond to a Gaussian distribution, centered at $\widetilde{\Lambda}_{obs} = 400$ with a dispersion of $\sigma_{\widetilde{\Lambda}} = 243$. We also use the inferred chirp mass from GW170817, which is constrained to $\mathcal{M}_c = 1.188^{+0.004}_{-0.002}\ M_\odot$.

The likelihood of a particular EOS is given by

$$P(\text{EOS}|\mathcal{M}_c, \widetilde{\Lambda}) = P_{pr}(\text{EOS})P(\mathcal{M}_c, \widetilde{\Lambda}|\text{EOS}), \qquad (13)$$

where $P_{pr}(\text{EOS})$ represents the set of the priors on the EOS, which we describe above. Because of the high accuracy in the measurement of the chirp mass, we fix it to the observed value, and use that to set m_2 for any given m_1. Then, Equation (13) can be written as

$$P(\text{EOS}|\widetilde{\Lambda}) = P_{pr}(\text{EOS})$$
$$\times \frac{1}{\sqrt{2\pi}\,\sigma_{\widetilde{\Lambda}}} \exp\left\{ -\frac{[\widetilde{\Lambda}_{\text{EOS}(m_1,m_2)} - \widetilde{\Lambda}_{obs}]^2}{2\sigma_{\widetilde{\Lambda}}^2} \right\}, \qquad (14)$$

where $\widetilde{\Lambda}_{\text{EOS}(m_1,m_2)}$ is the effective tidal deformability for a particular set of the two masses, m_1 and m_2, of each EOS that maximizes the likelihood. We choose to use the maximum likelihood, rather than integrating over all combinations of m_1
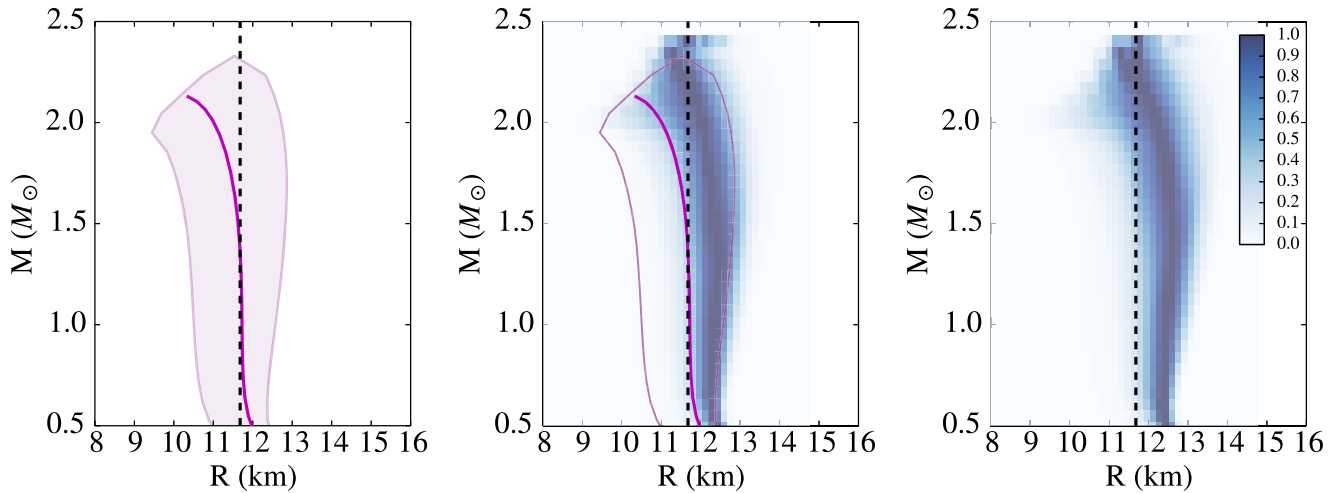
Figure 3. Left: mass–radius relations corresponding to the most-likely EOS in our Bayesian inference, with a sample distribution for $\widetilde{\Lambda}$ centered at $\widetilde{\Lambda} = 400$ and a fixed chirp mass of $\mathcal{M}_c = 1.188\,M_\odot$. The solid magenta line corresponds to the most-likely EOS, while the pink band corresponds to the range of EOS with posteriors within $1/\sqrt{e}$ of the maximum value. The black dashed line shows the analytic prediction from our $\widetilde{\Lambda} - R$ relation of Equation (9). We find excellent agreement between our $\widetilde{\Lambda} - R$ prediction and the full Bayesian inference. Middle: same as the left panel, but showing, in addition, the marginalized posteriors over the neutron star radii for a fixed grid of masses. These marginalized likelihoods are shown in blue. By marginalizing the posteriors in this way, the results are skewed to higher radii and away from the maximum-likelihood solution. Right: marginalized likelihoods for an inference with only the priors and no data. These marginalized posteriors are nearly identical to the marginalized posteriors from the inference that incorporated data from a $\widetilde{\Lambda} = 400$ centered Gaussian. This method of marginalization overweights the prior on the EOS pressures imposed by the observation of a $1.97\,M_\odot$ neutron star. The results of the marginalization are less sensitive to the input data and are not reliable.

and m_2 to avoid biasing our results, as discussed in Raithel et al. (2017).

To populate the posteriors in Equation (14), we run a Markov Chain Monte Carlo (MCMC) simulation with $\sim 10^6$ points. For each EOS that is tested in our MCMC, we also calculate the corresponding mass–radius relation using the standard TOV equations. In the left panel of Figure 3, we show the mass–radius relations corresponding to the highest-likelihood solutions from our MCMC. The solid magenta line shows the most likely solution, while the pink shaded band corresponds to the range of EOS with probabilities within $1/\sqrt{e}$ of the maximum value. Figure 3 also shows, as the black dashed line, the radius that corresponds to the most likely value of $\widetilde{\Lambda} = 400$ using the quasi-universal relation of Equation (9). Both our analytic expansion of the $\widetilde{\Lambda}$-radius relationship and the full Bayesian inference presented here imply radii of ~ 11.7 km, for these sample data. This Bayesian method can be used to robustly infer the EOS as additional measurements of $\widetilde{\Lambda}$ and $\mathcal{M}_c$ are made from future neutron star merger events.

As a note of caution, we show in the middle and right panels of Figure 3 the results of our MCMC after they have been marginalized in mass–radius space, as is frequently presented in some other studies (e.g., Steiner et al. 2017; Most et al. 2018). This method of marginalization involves calculating the posteriors over radius in a fixed grid of masses. However, because there are far more large-radii EOS that produce a $2\,M_\odot$ neutron star, marginalizing in this way effectively weights the large-radii solutions much more heavily than any other priors, or even than the data. This can be seen in the middle panel of Figure 3, which shows that the marginalized solution leads to an inferred radius of ~ 12.2 km, even though the maximum-likelihood solution occurs at ~ 11.7 km. To further illustrate the point, we show in the right panel of Figure 3 the marginalized posteriors for an inference with only priors and no data at all. The marginalized posteriors with no

data are effectively identical to the marginalized posteriors for the inference that incorporated data from a $\widetilde{\Lambda} = 400$ centered Gaussian. This method of marginalization weights the $2\,M_\odot$ prior so heavily that the data are effectively ignored. We suspect that this bias also affects the posteriors presented in other works, e.g., Most et al. (2018). For further discussion of the bias introduced by such a marginalization, see Raithel et al. (2017).

6. Conclusions

In this Letter, we found that the effective tidal deformability is approximately independent of the component masses for a neutron star–neutron star merger, when the chirp mass is specified. Because this surprising result is difficult to see analytically in the fully relativistic case, we introduce a quasi-Newtonian approximation that closely reproduces the results found in full general relativity. In the quasi-Newtonian limit, we find that the masses of the stars only enter at order $\mathcal{O}((1-q)^2)$, where q is the mass ratio. We find that, for the chirp mass measured from GW170817, this introduces at most a 4% mass correction to the effective tidal deformability for the entire range of mass ratios. Thus, the effective tidal deformability can be considered as approximately independent of the neutron star masses. This makes $\widetilde{\Lambda}$ a direct probe of the neutron star radius. For GW170817, we find that the 90% upper limit on $\widetilde{\Lambda}$ implies that the neutron star radius must be $\lesssim 13$ km.

In the case of a neutron star–black hole merger, we find that the vanishing Λ for the black hole breaks the symmetry in $\widetilde{\Lambda}$ and makes it depend more strongly on the component masses. Thus, a measurement of $\widetilde{\Lambda}$ for a neutron star–black hole merger probes the compactness of the neutron star, but cannot be used as a direct probe of the radius.

Finally, we incorporate other astrophysical priors and constraints from nuclear physics in order to perform an example Bayesian inference of the pressures in a parametric EOS, from the $\mathcal{M}_c$ value inferred in GW170817 and a sample

interpretation of the reported upper limit on $\widetilde{\Lambda}$. We find that, even when such priors are included, we infer a mass–radius relation that is consistent with the analytic prediction from our $\widetilde{\Lambda} - R$ universal relationship. We show that significant biases can be avoided by robustly examining the maximum-likelihood solutions in the multi-dimensional parameter space, rather than introducing a marginalization in mass–radius space. The marginalization tends to weight particular priors more heavily than the actual data, which causes the resulting answer to skew systematically toward larger radii.

Using the methods we have developed in this Letter, future gravitational-wave events can be used to directly and robustly constrain the neutron star radius, providing new constraints on the EOS.

ORCID iDs

Carolyn A. Raithel ⬤ https://orcid.org/0000-0002-1798-6668
Dimitrios Psaltis ⬤ https://orcid.org/0000-0003-4058-2837

References

Abbott, B. P., Abbott, R., Abbott, T. D., et al. 2017a, PhRvL, 119, 161101
Abbott, B. P., Abbott, R., Abbott, T. D., et al. 2017b, ApJL, 848, L12
Antoniadis, J., Freire, P. C. C., Wex, N., et al. 2013, Sci, 340, 448
Arun, K. G., Buonanno, A., Faye, G., & Ochsner, E. 2011, PhRvD, 84, 049901
Berger, E. 2014, ARA&A, 52, 43
Binnington, T., & Poisson, E. 2009, PhRvD, 80, 084018
Bohé, A., Faye, G., Marsat, S., & Porter, E. K. 2015, CQGra, 32, 195010
Bohé, A., Marsat, S., & Blanchet, L. 2013, CQGra, 30, 135009
Damour, T., & Nagar, A. 2009, PhRvD, 80, 084035
Eichler, D., Livio, M., Piran, T., & Schramm, D. N. 1989, Natur, 340, 126
Favata, M. 2014, PhRvL, 112, 101101
Flanagan, É. É., & Hinderer, T. 2008, PhRvD, 77, 021502
Fonseca, E., Pennucci, T. T., Ellis, J. A., et al. 2016, ApJ, 832, 167
Hinderer, T. 2008, ApJ, 677, 1216
Hinderer, T., Lackey, B. D., Lang, R. N., & Read, J. S. 2010, PhRvD, 81, 123016
Kawaguchi, K., Kiuchi, K., Kyutoku, K., et al. 2018, PhRvD, 97, 044044
Lackey, B. D., Nayyar, M., & Owen, B. J. 2006, PhRvD, 73, 024021
Lackey, B. D., & Wade, L. 2015, PhRvD, 91, 043002
Li, L.-X., & Paczyński, B. 1998, ApJL, 507, L59
Margalit, B., & Metzger, B. 2017, arXiv:1710.05938
Metzger, B. D., Martínez-Pinedo, G., Darbha, S., et al. 2010, MNRAS, 406, 2650
Mikóczi, B., Vasúth, M., & Gergely, L. Á. 2005, PhRvD, 71, 124043
Mishra, C. K., Kela, A., Arun, K. G., & Faye, G. 2016, PhRvD, 93, 084054
Most, E. R., Weih, L. R., Rezzolla, L., & Schaffner-Bielich, J. 2018, arXiv:1803.00549
Müller, H., & Serot, B. D. 1996, NuPhA, 606, 508
Narayan, R., Paczynski, B., & Piran, T. 1992, ApJL, 395, L83
Özel, F., & Freire, P. 2016, arXiv:1603.02698
Özel, F., & Psaltis, D. 2009, PhRvD, 80, 103003
Postnikov, S., Prakash, M., & Lattimer, J. M. 2010, PhRvD, 82, 024016
Raithel, C. A., Ozel, F., & Psaltis, D. 2016, arXiv:1605.03591
Raithel, C. A., Özel, F., & Psaltis, D. 2017, ApJ, 844, 156
Read, J. S., Baiotti, L., Creighton, J. D. E., et al. 2013, PhRvD, 88, 044042
Read, J. S., Lackey, B. D., Owen, B. J., & Friedman, J. L. 2009a, PhRvD, 79, 124032
Read, J. S., Markakis, C., Shibata, M., et al. 2009b, PhRvD, 79, 124033
Rezzolla, L., Most, E. R., & Weih, L. R. 2017, arXiv:1711.00314
Sathyaprakash, B. S., & Dhurandhar, S. V. 1991, PhRvD, 44, 3819
Steiner, A. W., Heinke, C. O., Bogdanov, S., et al. 2017, arXiv:1709.05013
Vines, J., Flanagan, É. É., & Hinderer, T. 2011, PhRvD, 83, 084051
Wade, L., Creighton, J. D. E., Ochsner, E., et al. 2014, PhRvD, 89, 103012
Yagi, K., & Yunes, N. 2013, PhRvD, 88, 023009
Yagi, K., & Yunes, N. 2017, PhR, 681, 1